



Hydrogeology of a montane headwater groundwater system downgradient of a coal-mine waste rock dump: Elk Valley, British Columbia, Canada

Jakub T. Szmigielski¹ · S. Lee Barbour² · Sean K. Carey³ · John Kurylo⁴ · A. F. McClymont⁵ · M. Jim Hendry¹

Received: 15 October 2017 / Accepted: 23 May 2018 / Published online: 16 June 2018
© Springer-Verlag GmbH Germany, part of Springer Nature 2018

Abstract

Steelmaking-coal waste rock placed in mountain catchments in the Elk Valley, British Columbia, Canada, drain constituents of interest (CIs) to surface water downgradient of the waste rock dumps. The role of groundwater in transporting CIs in the headwaters of mountain catchments is not well understood. This study characterizes the physical hydrogeology of a portion of a 10-km² headwater catchment (West Line Creek) downgradient of a 2.7-km² waste rock dump placed over a natural headwater valley-bottom groundwater system. The study site was instrumented with 13 monitoring wells. Drill core samples were collected to determine subsurface lithology and geotechnical properties. The groundwater system was characterized using field testing and water-level monitoring. The valley-bottom sediments were composed of unconsolidated glacial and meltwater successions (<64 m thick) deposited as a series of cut and fill structures overlying shale bedrock. An unconfined basal alluvial aquifer located above fractured bedrock was identified as the primary conduit for groundwater flow toward Line Creek (650 m from the toe of the dump). Discharge through the basal alluvial aquifer was estimated using the geometric mean hydraulic conductivity (± 1 standard deviation). These calculations suggest groundwater discharge could account for approximately 15% (ranging from 2 to 60%) of the total water discharged from the watershed. The residence time from the base of the waste rock dump to Line Creek was estimated at <3 years. The groundwater system was defined as a snowmelt (i.e., nival) regime dominated by direct recharge (percolation of precipitation) across the catchment.

Keywords Mining · Canada · Coal · Headwater mountain catchment · Physical hydrogeology

Electronic supplementary material The online version of this article (<https://doi.org/10.1007/s10040-018-1809-z>) contains supplementary material, which is available to authorized users.

✉ Jakub T. Szmigielski
jas676@mail.usask.ca

S. Lee Barbour
lee.barbour@usask.ca

Sean K. Carey
careysk@mcmaster.ca

John Kurylo
j.kurylo@srk.com

A. F. McClymont
alastairmcclymont@gmail.com

M. Jim Hendry
jim.hendry@usask.ca

¹ Department of Geological Sciences, University of Saskatchewan, Saskatoon, SK, Canada

² Department of Civil, Geological and Environmental Engineering, University of Saskatchewan, Saskatoon, SK, Canada

³ School of Geography and Earth Sciences, McMaster University, Hamilton, ON, Canada

⁴ SRK (Canada) Consulting Inc., Vancouver, BC, Canada

⁵ Worley Parsons Canada Ltd., Calgary, AB, Canada

Introduction

The Elk Valley watershed, located in the mountainous East Kootenay region of southeastern British Columbia (BC) (Fig. 1), is a major source of steel-making coal in Canada. A multi-disciplinary research program is underway to improve upon the understanding of the origin, fate, and transport of constituents of interest (CIs; including selenium [Se], sulfate [SO₄²⁻], and nitrate [NO₃⁻]) derived from coal-mine waste rock to the Elk River (Fig. 1). Exposure of waste rock to atmospheric conditions during blasting and dump placement causes sulfide minerals present in the rock (e.g. pyrite) to oxidize producing sulfuric acid (H₂SO₄). Carbonate minerals present in the rock buffer the acid; however, the weathering process still results in the release of CIs incorporated in the sulfide minerals (Se and SO₄²⁻). Nitrate (NO₃⁻) is released from explosives during mining and can also leach from the waste rock into receiving waters (Mahmood et al. 2016). Waste rock dumps in the valley can be up to several kilometers long and hundreds of meters high (Wellen et al. 2015). Although the impact of the waste rock on surface-water quality and catchment hydrology in the Elk Valley has been studied (Shatilla 2013; Villeneuve et al. 2017; Wellen et al. 2015), CI migration via groundwater is not well understood in headwater catchments.

Miller and Zégre (2014) demonstrate that the placement of waste rock from shallow coal-seam mining in the United States can alter the catchment landscape, vegetation, and surface runoff pathways. The impacts of coal mining on downstream surface-water systems are well documented (Bernhardt and Palmer 2011; Griffith et al. 2012; Miller and Zégre 2014), but complex and poorly defined hydrogeology has made delineating CI release through groundwater difficult (Holzman 2011). In the Powder River Basin in Wyoming, limited data provide insight into the contribution of CIs (e.g. Se, SO₄²⁻, and NO₃⁻) in groundwater to water quality downstream of waste rock dumps (Dreher and Finkelman 1992; Everett 1985; Naftz and Rice 1989).

Mountain catchments are high relief environments that are important sources of freshwater for local ecosystems and connected downstream basins (Allen 2011; Viviroli and Messerli 2003). The hydrogeology of arid and semi-arid continental mountain catchments of the western United States has been characterized (Ajami et al. 2012; Manning and Solomon 2003, 2005; Wahi et al. 2008; Wilson and Guan 2004). There is comparatively less hydrogeological information in northern temperate mountainous regions such as the Canadian Cordillera (Allen et al. 2010), and in particular headwater catchments. The hydrogeology of these environments is poorly understood (Tiedeman et al. 1998; Viviroli et al. 2007; Winter et al. 2003) and studies have relied on surface-water characterization or runoff measurements (i.e., springs, lakes, and ponds) to elucidate water sources and groundwater flow

paths (cf. Clow et al. 2003). This is due in part to the difficulty of drilling boreholes and installing wells in these areas given limited access and regulations regarding the protection of pristine environments (Roy and Hayashi 2009). Mining operations in the Elk Valley have developed conceptual models of local groundwater flow systems and a regional groundwater model was developed for the Elk River floodplain (i.e., lowland areas; Teck Resources Ltd. 2017).

The objectives of this study were to characterize the physical hydrogeology of a headwater catchment in the Elk Valley and the effect(s) of waste rock placement on the local valley-bottom groundwater system. The objectives were met by installing and monitoring (over a 2-year study period) 13 wells in the water-bearing formations and collecting and analyzing core samples to define subsurface lithology and geotechnical properties. These data were augmented with spatial geophysical measurements. The interpretation of the groundwater flow system was integrated with observations of watershed hydro-meteorology as well as flow and chemistry from a rock drain (a permeable rubble zone at the base of the dump) as reported by Barbour et al. (2016) and Villeneuve et al. (2017). These data allowed one to estimate the rates and fluxes of groundwater discharging from the catchment. The findings of this study provide a unique case history of water migration from coal-mine waste rock dumps, through the groundwater regime, and into the surface water. It also improves upon the limited understanding of the hydrogeology of headwater catchments in northern temperate mountainous regions.

Materials and methods

Study area

The study area is located in the small (10 km²) West Line Creek (WLC) catchment situated approximately 25 km north of Sparwood, in southeastern BC, Canada (Fig. 1). The catchment is a part of the Line Creek Operation (LCO) operated by Teck Resources Ltd. The mine site drains several small catchments adjacent to Line Creek, a tributary of the Elk River. The WLC catchment ranges in elevation from 1,450 to 2,650 m above sea level (m asl) at the peaks of the Wisukitsak range (Shatilla 2013). A series of five alpine cirques occur between the limestone and sandstone peaks along the western edge of the catchment (Fig. 2a). The orientation of the valley (i.e., the centerline azimuth) is approximately 160° and roughly parallels the crest of the eastern edge of the catchment.

The valley has a U-shaped cross section, indicative of its glacial origin, and the slopes of the valley walls progressively steepen with increasing elevation above the creek. Geomorphological processes on the valley walls produced large-scale downslope movement of colluvium or talus slopes. A series of ephemeral streams have cut deep (>15 m) channels

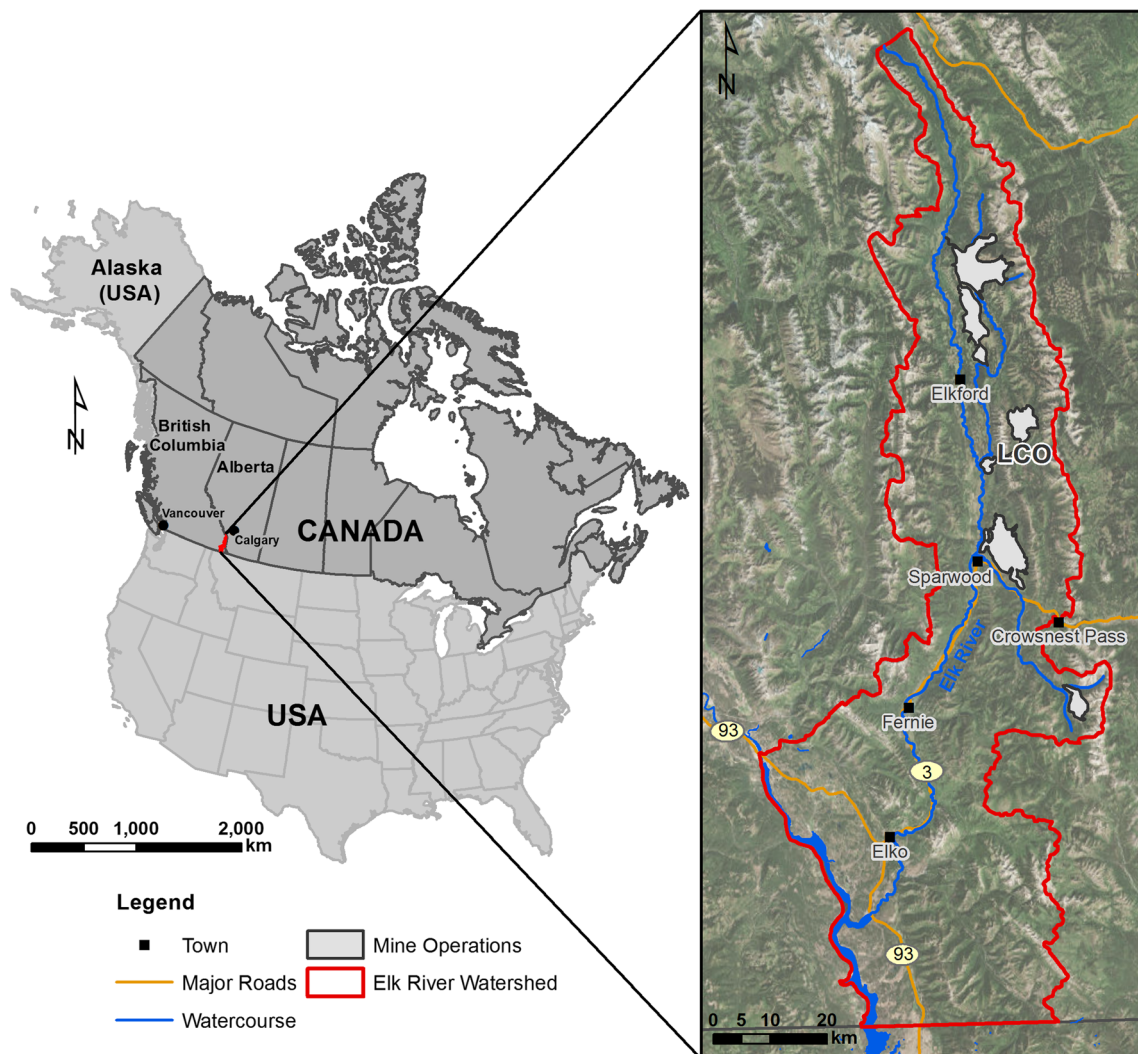


Fig. 1 Location of the Elk Valley, British Columbia, Canada, and coal mining operations in the valley, including the Line Creek Operation (LCO)

into the colluvium. The bedrock unit at the base of the valley is the Fernie shale Formation into which the historical WLC stream cut a 300-m ravine prior to valley infilling (Golder Geotechnical Consultants (now Golder Associates Ltd.) 1979). Butrenchuk (1987) states that the Fernie Formation in the WLC catchment dips steeply eastward, with the base of this unit outcropping along the western slopes of the catchment. Riddell (2012) and Michael and Bachu (2001) define the Fernie Formation as a regional aquitard.

The mean annual temperature at Sparwood, BC is approximately 4 °C (9–15 °C in summer and –2 to –7 °C in winter). The mean annual precipitation reported at the Sparwood (Fig. 1) Environment Canada (2017) station (weather station ID 1157630; elevation 1,137 m asl) is 772 mm. Two on-site weather-monitoring stations measured mean annual precipitation ranging from 600 to 800 mm (2012–2014), although these values might not be representative of the entire catchment given the wide range of elevations in the watershed. For example, Shatilla (2013) reports that from 1,300 to 1,850 m

asl the proportion of snow to rain in 2012 varied from 28 to 66% and Barbour et al. (2016) uses a precipitation lapse rate of +21 mm/100 m to estimate climatic conditions over the range of elevations at the WLC dump.

The WLC waste rock dump was constructed between 1981 and 2012 using end-dump methods. It covers about 30% of the catchment (2.7 km²) along its eastern extent (Fig. 2a). In 2010, the waste rock dump was approximately 3.5 km long and 1 km wide with a mean thickness of 115 m and a total volume of approximately 2.1×10^8 m³ (Villeneuve et al. 2017). End-dumping has caused coarser material to segregate on the valley floor and form a cobble rich zone (rock drain) over the historical stream course. Barbour et al. (2016) evaluated the seasonality and magnitude of net percolation into the WLC waste rock dump and the downgradient natural alluvial deposits using high resolution vertical profiles of stable isotopes of water ($\delta^2\text{H}$ and $\delta^{18}\text{O}$). The ranges of $\delta^2\text{H}$ and $\delta^{18}\text{O}$ in pore water and water samples from the rock drain suggest the rates of recharge through the unreclaimed dumps is two to

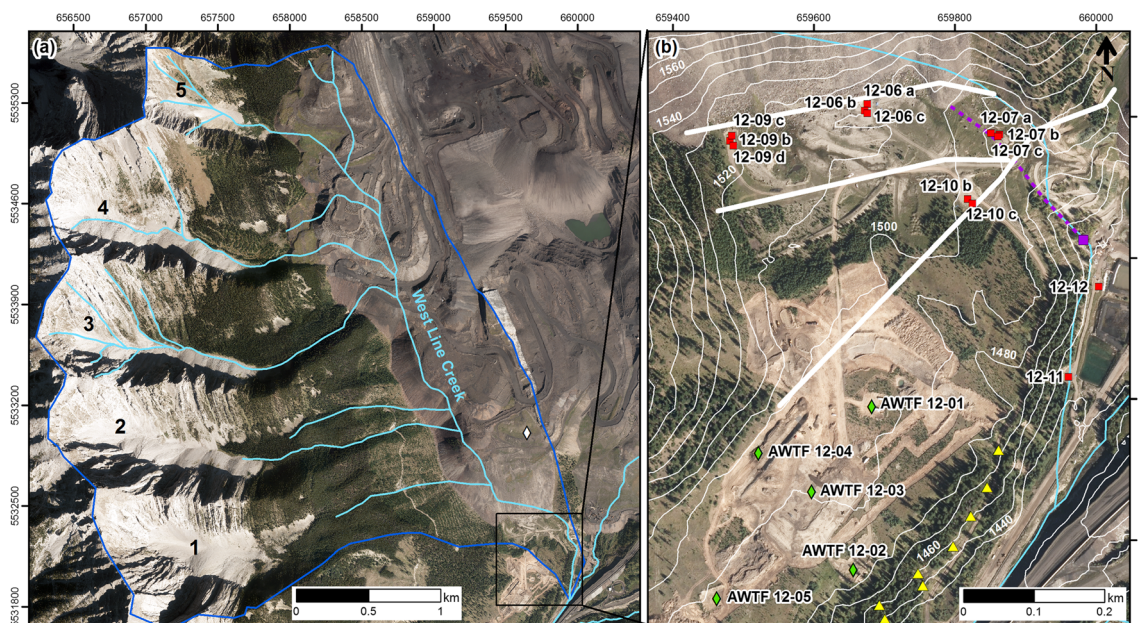


Fig. 2 The study area: **a** study area location (black box) within the West Line Creek watershed showing the five west-valley cirques (numbered) and the meteorological station at the southern extent of the waste rock dump (white diamond); and **b** a topographic map of the study area (10-m elevation contours) showing the location of boreholes drilled as part of the current study (red squares), the electrical resistivity survey (thick white

lines), five boreholes drilled as part of the active water treatment facility technical study (green diamonds), groundwater springs (yellow triangles), and the subsurface drainage culvert that collects and transmits rock drain water (dashed purple line) toward the culvert outlet (purple square) from 1,500 to 1,450 m asl. Map coordinates displayed as NAD 1983 UTM Zone 11 N

three times that of natural, vegetated slopes. The volume of recharge into the dump was equally distributed between snowmelt and summer rainfall. Villeneuve et al. (2017) also estimated greater net percolation through the dump than through the natural watershed (from 1.5 to 5 times) based on time-series CI concentrations from the rock drain.

The valley-bottom downslope of the waste rock dump is a gently sloping terrace approximately 1 km long (Fig. 2b). LiDAR data collected since mining commenced suggest the topography of this terrace has remained largely unchanged following dump placement. A steep slope at the SE boundary demarks the terminus of the catchment where it joins with the larger Line Creek drainage (Fig. 2b). A corrugated pipe drainage culvert, referred to as the rock drain culvert, was buried in the terrace sediments to direct water from the rock drain toward Line Creek. The location of the rock drain culvert that extends from the toe of the waste rock dump towards the southeast (Fig. 2b) was confirmed using a magnetic survey. Golder Geotechnical Consultants (now Golder Associates Ltd.) (1979) report that the culvert was constructed on top of coarse debris placed within the existing WLC creek channel to accommodate greater flow volumes.

Drilling

Thirteen boreholes were drilled at six sites over the southern extent of the WLC catchment between July and August 2012 (Fig. 2b). All boreholes were drilled using either sonic (drilled

without the use of water) or air rotary drill rigs (Table 1). The boreholes were typically drilled in nests of two to three holes to target different aquifers at the same location. Sonic drilling was performed using a Boart Longyear (Sonic Rig 1524) truck-mounted sonic drill rig with a 152–178-mm casing. Sonic core samples were collected using a 0.10-m ID (and occasionally 0.15-m ID) \times 3.05-m-long core barrel with approximately 90% core recovery. These boreholes were drilled and continuously cored to depths ranging from 12.8 to 56.4 m below ground surface (bgs). Air rotary boreholes were drilled using a JR Drilling (Foremost DR 24 drill) truck-mounted air rotary rig with a 152–203-mm casing. These boreholes were drilled to depths ranging from 9.3 to 76.3 m bgs. Drill cuttings from the air rotary drilling were logged for physical and lithological characteristics in the field, while sonic core was transferred to an on-site core shed for logging and sampling.

Duplicate samples were collected from the sonic core at approximately 1-m intervals. Sample handling methods were designed to preserve samples for subsequent physical, chemical, and isotopic analyses reported in companion studies (e.g., Barbour et al. 2016; Hendry et al. 2015). After retrieval of the core barrel, the core sample was transferred into a plastic sleeve. The ends of the sleeves were immediately knotted, placed in a 101.6-mm-diameter polyvinyl chloride (PVC) half pipe, and transferred to the on-site core shed. In the shed, the sleeves were cut lengthwise, the cores were logged, and solids samples collected. Prior to collecting samples, the outer 1–5-mm layer of the core was removed to minimize sample

Table 1 Details of drilling program

Borehole ID	Surface elevation (m asl)	Total depth (m bgs)	Depth range of screened interval (m bgs)	Geologic formation
Sonic boreholes				
LC-WLC-12-06a	1,509.8	44.2	10.7–13.7	Overburden
LC-WLC-12-06b	1,509.9	25.9	19.8–22.9	Overburden
LC-WLC-12-07a	1,489.1	12.8	10.2–11.3	Bedrock
LC-WLC-12-09b	1,524.1	46	41.2–44.2	Overburden
LC-WLC-12-10b	1,498.3	56.4	44.2–47.2	Overburden
LC-WLC-12-11	1,442.4	28	3.7–6.7	Overburden
LC-WLC-12-12	1,447.5	32	21.1–24.1	Overburden
Air rotary boreholes				
LC-WLC-12-06c	1,509.8	76.2	72.5–75.6	Bedrock
LC-WLC-12-07b	1,488.7	16.8	11.4–14.3	Bedrock
LC-WLC-12-07c	1,488.6	9.3	6.2–7.8	Overburden
LC-WLC-12-09c	1,524.3	47.4	34.1–40.2	Overburden
LC-WLC-12-09d	1,523.6	11	6.1–9.1	Overburden
LC-WLC-12-10c	1,497.6	65.8	60.7–63.7	Bedrock

contamination. All core samples were immediately transferred into double 1-L Ziploc plastic bags with the air squeezed out prior to sealing and placed in a cooler for transport off-site. The following day, the core samples were transferred from the Ziploc bags into double Food Saver bags (0.20 m × 0.23 m) and vacuum sealed. The Food Saver bags were weighed and stored at room temperature prior to shipment to the Aqueous Environmental and Geochemistry Laboratory (AEG) at the University of Saskatchewan.

Monitoring well installation and downhole data logging

Monitoring wells were installed to target key water-bearing units (Table 1; Fig. 2b). The wells were constructed using either 51 or 102-mm Schedule 40 PVC with a PVC screen. All screens were 3.05 m in length with the following exceptions: two shallow wells (12-07a and 12-07c; Table 1; Fig. 2b) had 1.52-m intake screens and one well (12-09c; Table 1; Fig. 2b) had a 6.10-m intake screen. A sand pack was placed around the screened interval extending 0.61 to 1.52 m above the top of the screen. A bentonite seal (1.52–3.04 m) was typically placed above the top of the sand pack before the drill rods were pulled. Subsequently, the remainder of the annular space was filled with bentonite chips and pellets after the casing was removed. Select boreholes also had an additional segment of PVC placed below the screened interval to act as a sump for fine-grained sediments entering the screens.

The monitoring wells were developed by purging three or more well volumes from wells that recovered rapidly and a minimum of one well volume for lower permeability units. The purging was done using an electrical Grundfos Redi Flow 2 pump equipped with a single discharge tube. After

the wells were purged, a Solinst 3001 Levellogger Edge was installed at the base of the screened interval in each well to record total pressure and temperature every 15 min. The pressure sensor accuracy was $\pm 0.05\%$ full scale. Solinst 3001 Barologger Edges, with a pressure sensor accuracy of ± 0.05 kPa, were installed within the open riser (1-m depth) to record barometric pressure (BP) at each well nest. The hydraulic head was calculated using the total pressure readings and subtracting the barometric pressure. Hydraulic head data were collected for the 2013 hydrological year (October 1, 2012 to September 30, 2013) and 2014 hydrological year (October 1, 2013 to September 30, 2014). Manual measurements of water levels were conducted intermittently using a Solinst Model 101 P7 water-level meter to ensure the accuracy of the submerged level logger.

Data from five additional boreholes and associated monitoring wells installed as part of a geotechnical site characterization for an active water treatment facility (AWTF) landfill (SRK Consulting Inc. 2013; Fig. 2b) were used to augment interpretations in the current study. These wells were located directly south of the study site and on the terrace at the southernmost extent of the catchment.

Hydraulic testing

In situ rising head hydraulic conductivity (K) tests were conducted on wells with completely submerged screened intervals based on ASTM D4044–96 (2008). Drawdowns in the wells were induced using a Geotech SS Geosub electric pump. Water-level recoveries were measured at 1–60-s measurement intervals on a Solinst 3001 Levellogger Edge. Rising head tests were also conducted pneumatically in those wells screened in high- K units (i.e., exhibiting rapid water-level recovery)

following the method proposed by Butler et al. (2003). A well cap was modified to provide an airtight seal and compressed air was introduced into the well to depress the water level by approximately 0.5 m or less. The K values were determined using the method of Bouwer and Rice (1976) and software developed by Halford and Kuniandy (2002). Three or more rising head tests were conducted at each well using two or more different initial displacements (H_0) of the water column.

Geotechnical analyses

Particle size distribution, gravimetric water content (ω), and dry bulk density (ρ_d) measurements were performed on two subsamples from each 1 m of sonic drill core. Particle size analysis was performed using the ASTM D422–63 (2007) sieve-hydrometer method and a laser-diffraction method (LDM). Results of the LDM particle size analysis were calibrated to the sieve-hydrometer method as outlined in Eshel et al. (2002). Approximately 2 kg of each core were collected and homogenized in a steel bowl. Core samples were first sieved to determine gravel-sized fractions, and then analyzed by LDM to determine sand, silt, and clay fractions. The LDM analysis was performed using a Mastersizer 2000 and samples were run at a laser obscuration of 10 to 15%, dispersion pump speed of 2,200 rpm, and ultrasonic tip displacement of 3 μm for 60 s prior to data collection. Each sample was measured three times for 20 s, with the mean of the three runs reported (Sperazza et al. 2004). Particle sizes are presented using the United States Department of Agriculture (USDA) classification for soil particles (<2- μm clay, 2–50- μm silt, 50–2,000- μm sand, and >2,000- μm gravel).

Sonic drill core subsamples were weighed before the sealed sample bags were opened to ensure no water loss occurred during storage. The ω values of core samples were determined using ASTM D2216–10 (2010) on 40–80 g of sediment collected from each sample bag. The ρ_d values of core samples were determined using ASTM D7263–09 Method A (2009). Measurements were only performed on samples that remained sufficiently intact to form a >20-g clump and were dipped in liquid paraffin wax (density = 0.85 g/cm³). Subsequently, the total porosities (n_T) of core samples were estimated using the measured ρ_d values and an assumed particle density (S_g ; 2.7 g/cm³) similar to ASTM D7263–09 Appendix X1 (2009).

Electrical resistivity tomography

An electrical resistivity tomography (ERT) survey was conducted along three 400–800-m-long profiles (Fig. 2b). For each line, minimum electrode intervals of either 5 m or 10 m were used resulting in a maximum depth of investigation of either 60 or 120 m bgs, respectively. Raw data were recorded with an ABEM Terrameter LS system using a modified gradient array configuration (Zonge et al. 2005). The datasets

were processed using commercially available RES2DINV tomography software, which is based on an iterative, smoothness-constrained least squares inversion algorithm (Loke and Dahlin 2002). Subsurface features, in particular the overburden-bedrock contact, were mapped by correlating drilling logs with structures identified in the ERT sections using Mira GOCAD software (Mira Geosciences Ltd. 2009).

Discharge measurements at groundwater springs and the rock drain

Discharge measurements from groundwater springs and drainage culverts proximal to springs (Fig. 2b) were made multiple times each year using a bucket and stopwatch. Visual inspection of the springs on a bimonthly (fall and winter) and biweekly (spring and summer) basis allowed annual maximum and minimum flow rates to be determined. A flume constructed from PVC was used to capture and direct water toward a 19-L bucket.

Discharge measurements were conducted at the rock-drain culvert outlet (Fig. 2b) by McMaster University (e.g., Shatilla 2013) and Teck Resources Ltd. personnel using a SonTek Flowtracker and the velocity-area stream gauging method to develop a stage-discharge rating curve. This rating curve was then applied to the water-level measurements made using the levelogger to estimate discharge in 15-min intervals. Water-level measurements were obtained using a submerged Solinst 3001 Levelogger Edge pressure transducer. A Solinst 3001 Barologger Edge was installed in an enclosure adjacent to the culvert outlet to record BP to subtract from total pressure readings of the Levelogger.

Air temperature and precipitation

A meteorological station recorded air temperatures and precipitation at the southernmost extent of the waste rock dump on a flat revegetated site at 1,803 m asl (Fig. 2a). Rainfall was recorded every 30 min using a Campbell Scientific CS700 tipping bucket rain gauge. A Geonor T-200B all-weather precipitation weighing gauge recorded total precipitation (i.e., rainfall + snowfall) every 30 min. Annual precipitation estimates for the 2013 (October 1, 2012 to September 30, 2013) and 2014 (October 1, 2013 to September 30, 2014) hydrological years were determined based on a combination of Geonor weighing gauge (snowfall) and tipping bucket rain gauge (rainfall) data.

³H/³He groundwater sampling and analysis

Samples for ³H/³He were collected at three monitoring wells in August 2013. Tritium samples (³H) were collected using a Geotech SS Geosub electric pump following a method similar to Gardner and Solomon (2009). Helium-3 samples (³He)

were collected in situ using a passive diffusion sampler made from a refrigeration grade copper tube attached to a semi-permeable membrane. A full description of the $^3\text{H}/^3\text{He}$ sampling method is provided in Appendix A in the electronic supplementary materials (ESM). The $^3\text{H}/^3\text{He}$ samples were analyzed by the Dissolved Gas Service Center Laboratory, University of Utah.

Results and discussion

Unconsolidated overburden sediment geology

Three major lithologic units were identified during drilling of the unconsolidated overburden sediments (8–53-m thick): glacio-fluvial, glacio-lacustrine, and glacial till. Soil textures ranged from poorly sorted sandy-silt to well-sorted gravel materials based on drill logs and particle size analyses of core samples ($n = 125$). Soil textures changed abruptly with depth in individual boreholes and horizontally between adjacent boreholes. The drill logs (simplified according to major divisions of the United Soil Classification System) and results of particle size analyses at boreholes nests 12-06 and 12-07 are presented in Fig. S1 of the electronic supplementary material (ESM).

The glacio-fluvial sediments were the dominant overburden lithology and present as numerous subsurface paleochannels evidenced by high resistivity regions ($>500 \Omega\text{m}$) in the ERT surveys (denoted by “p” and shown from a 3-D perspective in Fig. S2 of the ESM). These observations are consistent with a depositional environment of braided streams depositing substantial bedload at the lower end of the catchment’s fluvial plain. Gravel-sized particles comprised as much as 84% of the core samples at some depths (borehole 12-11; Table 1; Fig. 2b). Their presence is consistent with the transport of large sediment loads by streams receiving meltwater from both advancing and retreating glaciers that commonly produce braided streams (Rosenshein 1988). Coarse-grained sediments containing cobbles and boulders (observed in drill core) are also consistent with ice-contact deposits reflecting the late glacial history of the catchment.

A fine-grained sediment interval consisting of clay and silt was encountered at depths ranging from 4 to 15 m bgs at the upper elevation borehole nests (i.e., 12-06, 12-07, 12-09, and 12-10; Table 1; Fig. 2b). This interval was described as a medium-to-highly plastic clay to silty-clay unit of glacio-lacustrine origin. Laminations observed within this layer in both drill core and field reconnaissance of access road-cuts are evidence that this unit is of lacustrine origin (De Geer 1912). The presence of lacustrine sediments suggests that there was a relatively quiescent depositional period at the

study site, likely as a result of outflow from the catchment being restricted due to the outlet being dammed.

A poorly sorted sediment interval was observed near the base of boreholes 12-06, 12-11, and 12-12 (Table 1; Fig. 2b) and was interpreted as a basal till. Glacial tills are commonly encountered in valleys formed by glaciers. The glacial till was laterally discontinuous. The absence of till from some boreholes is in keeping with the cut and fill nature of the valley overburden, which is narrower than the overall valley and produced by glacial advancement and retreat (Jorgensen and Sandersen 2006). These cut and fill structures can produce truncated facies associations and complex fill successions that can be difficult to correlate (Russell et al. 2004). A discrete layer of clays and silts was occasionally encountered directly above the overburden-bedrock contact, separating the two lithologies.

The mean n_T ($\pm\text{SD}$) values of glacio-fluvial, glacio-lacustrine, and glacial till sediments were determined from ω and ρ_d measurements (data not presented) to be $26 \pm 6\%$ ($n = 67$), $38 \pm 5\%$ ($n = 15$), and $33 \pm 6\%$ ($n = 37$), respectively. The n_T values of the glacio-lacustrine sediments were significantly greater than for the glacio-fluvial sediments. Notably, however, the fine-grained units were better represented because of the greater number of intact cores (i.e., $>20\text{-g}$ clumps) available for the more cohesive glacio-lacustrine deposits. The mean n_T of all core samples from the overburden deposits was $30 \pm 7\%$ ($n = 125$, range 16–49%).

Bedrock geology

Bedrock outcrops were examined along the eastern edge of the valley at 1,490 m asl and along the western edge at 1,507–1,514 m asl (identified in excavations during AWTF landfill construction). The outcrops were massive black, brown, and grey siltstone with brittle fractured zones and the occasional brown and oxidized sand interval. The drill core was of medium to high density, varying from brown to black with indications of weathering and fractures up to 18 m below the overburden–bedrock contact. These descriptions are consistent with the Fernie Formation, which is marine-deposited shale, siltstone, and sandstone (Golder Geotechnical Consultants (now Golder Associates Ltd.) 1979). Limited geotechnical analyses of drill core from the shale bedrock suggest an n_T ($n = 4$) of $20 \pm 4\%$, respectively. The estimate of n_T for the shale samples was the lowest of all the measured geologic units.

The elevation of the bedrock surface was defined using drilling logs and the two bedrock outcrop areas. The topography of the bedrock surface was developed by integrating these known elevations with the bedrock horizon interpreted on the ERT surveys (Fig. 3; Fig. S2 of the ESM). Bedrock was encountered in drill holes between 1,479 m asl in the NW (12-09c) and 1,416 m asl in the SE (12-11) (Table 1;

Fig. 3 Map of bedrock-overburden interface: **a** 4-m elevation contours (m asl) of the bedrock surface and **b** 10-m depth contours (m bgs) to top of bedrock (beneath overburden sediments). Also shown are boreholes drilled as part of the current study (red squares), boreholes (five) drilled as part of the active water treatment facility technical study (green diamonds), and bedrock outcrops (white crosses). Note: Cross sections A–A' and B–B' (black lines) are presented in Figs. S3 and S4 of the *ESM*

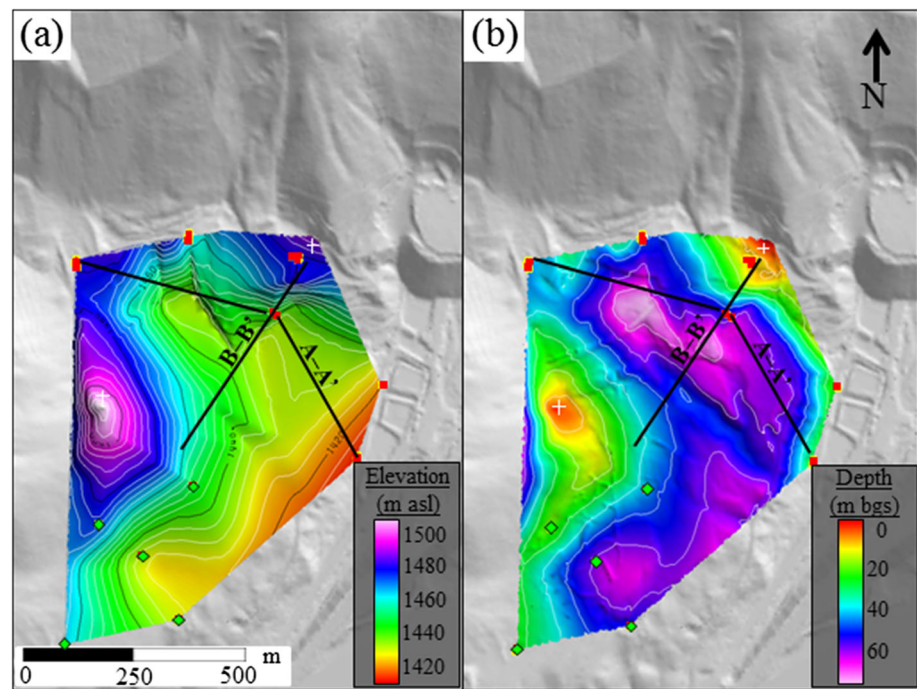


Fig. 2b; Fig. 3). The ERT surveys defined the overburden-bedrock contact by a change from moderate resistivities (generally greater than 300 Ωm) to an underlying bedrock layer associated with low resistivities that are generally less than 200 Ωm (Fig. S2 of the *ESM*). The bedrock contact from the ERT survey was as deep as 64 m bgs in the middle of the valley (see profile ERT-E in Fig. S2 of the *ESM*) and shallower on the sides of the valley. The bedrock surface also had a general dip towards the southeast. The U-shaped morphology of the valley is characteristic of glaciated montane valleys in the Western Cordillera (Heusser 1956).

Hydraulic testing

The estimated K values from the overburden monitoring wells ranged over more than two orders of magnitude (1.1×10^{-4} to 1.2×10^{-6} m/s) with a geometric mean of 3.4×10^{-5} m/s ($n = 6$; Table 2). These values might be an underestimation of the bulk K because the screened intervals of some monitoring wells were partially filled with fine-grained sediments (i.e., ‘silted in’; well 12-12) or had a broken well screen (well 12-09c; Table 1; Fig. 2b). The presence of these partially obstructed well screen intervals was attributed to poor well development, where pumping at high rates caused fine-grained sediments to migrate from the formation to the well (Driscoll 1986). In the case of a partially obstructed well screen, the unobstructed screen length was used to calculate K . Measurements of K in the AWTF wells ranged from 2×10^{-5} to 4×10^{-7} m/s (SRK Consulting Inc. 2013), suggesting the K in the overburden might range over more than three orders of magnitude across the study area. The large

variability of K reflects the heterogeneous texture of these overburden deposits.

The values for K in the two monitoring wells constructed in the bedrock were 1.4×10^{-8} and 7.6×10^{-8} m/s (Table 2). The estimated K value for 12-10c (Table 1; Fig. 2b) was considered less accurate because the screen interval was almost completely obstructed with fine-grained sediment. The measured K values are only representative of the upper weathered portion of the bedrock. Based on the relatively low estimates of K in the fractured bedrock compared with the overburden aquifers, the groundwater residence times in this unit are likely much greater than in the overlying overburden.

Hydraulic heads and rock drain flow

Seasonal variations in hydraulic head in the saturated overburden and fractured bedrock are shown in Fig. 4. Hydraulic head measurements showed a strong seasonal response to spring freshet in late May (up to 10.1 m), when mean daily air temperatures exceeded 0 °C, and also during large summer rainfall events. Flow in the rock drain also increased during the freshet and remained high (above base flow levels) throughout most of the summer; the peak discharge of up to 0.5 m³/s occurred in May–June and winter base flow was generally <0.05 m³/s. The rise in hydraulic heads in the wells was nearly coincident with the increase in flow from the rock drain, and the peak hydraulic heads occurred 5–13 days after maximum rock drain flow.

A 3- to 24-m thick unconfined aquifer was present above the low- K bedrock contact (8–53 m bgs) in the gravel paleochannels and glacial till sediments. This basal alluvial

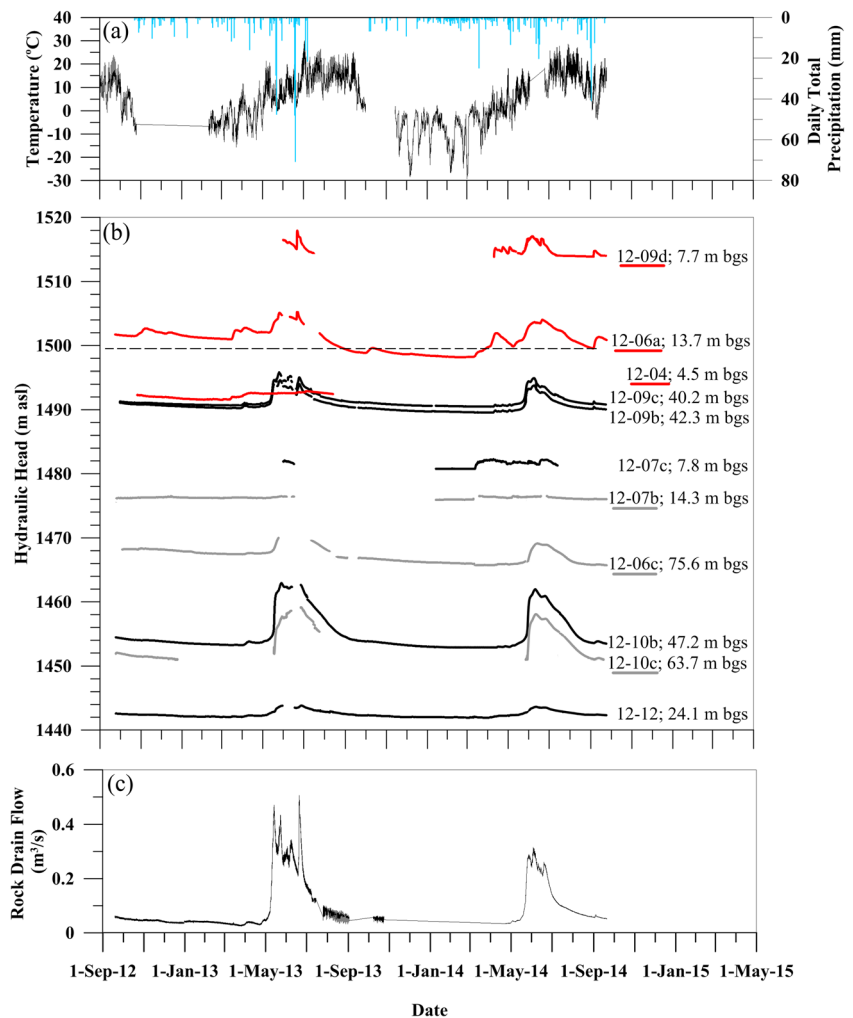
Table 2 Summary of results from rising head tests estimating the hydraulic conductivities (K) of monitoring wells with completely submerged screened intervals

Borehole	K_{min} (m/s)	K_{max} (m/s)	K_{mean} (m/s)	Geology	Comments
LCO-WLC-12-06a	1.0×10^{-4}	1.2×10^{-4}	1.1×10^{-4}	Overburden	–
LCO-WLC-12-09b	1.1×10^{-6}	1.4×10^{-6}	1.2×10^{-6}	Overburden	–
LCO-WLC-12-09c	5.9×10^{-5}	9.2×10^{-5}	7.5×10^{-5}	Overburden	Broken well screen
LCO-WLC-12-10b	2.7×10^{-4}	2.8×10^{-4}	2.8×10^{-4}	Overburden	–
LCO-WLC-12-11 N	1.2×10^{-4}	1.6×10^{-4}	1.3×10^{-4}	Overburden	–
LCO-WLC-12-12	3.7×10^{-6}	4.7×10^{-6}	4.3×10^{-6}	Overburden	Screened interval partially ‘silted in’
LCO-WLC-12-10c	6.9×10^{-8}	8.2×10^{-8}	7.6×10^{-8}	Bedrock	Screened interval completely ‘silted in’
LCO-WLC-12-06c	1.1×10^{-8}	1.6×10^{-8}	1.4×10^{-8}	Bedrock	–

aquifer was overlain by a thick unsaturated zone (7–45 m bgs). The greatest annual ranges in hydraulic head (9.4 and 10.1 m) were measured in the deep wells (12-09c, 12-10b; Table 1; Fig. 2b) located in the thalweg of the U-shaped bedrock surface. The mean saturated thickness of the aquifer, defined using water levels and the mapped bedrock surface,

was 12.4 and 10.0 m in wells 12-09c and 12-10b, respectively, increasing to a thickness of 22.9 m in the downgradient direction toward Line Creek (well 12-12; Table 1; Fig. 2b; Fig. S3 of the [ESM](#)). The saturated thickness thinned along the eastern periphery of the valley and the annual range in hydraulic head decreased to <1.6 m at well 12-07c (hydraulic head range of

Fig. 4 Summary of climate, groundwater hydraulic, and rock drain discharge data: **a** air temperature (solid line) and daily total precipitation (i.e., snowfall + rainfall; blue vertical bars); **b** hydrographs from the basal alluvial aquifer (black), perched aquifer (red), the bedrock formation (grey) shown with text (underlined with the corresponding color for perched and bedrock aquifer hydrographs) presenting the depth of the bottom of the screen intake zone (m bgs), with the dashed horizontal line indicating the intake elevation of the drainage culvert; and **c** rock drain discharge data. General note: Well 12-04 is located south of the study site in the AWTF area



1,482.3–1,480.7 m asl; Table 1; Figs. 2b and 4). Well 12-07c was dry for 8–9 months each year beginning in late summer. These observations suggest the vertical and lateral extent of the basal alluvial aquifer (i.e., the extent of saturated geologic materials) was controlled by the concave upward bedrock surface as well as the input of water following spring freshet and rainfall events.

A water-table contour map showing hydraulic head contours was generated for the basal alluvial aquifer using mean hydraulic heads measured in six wells (i.e., 12-07c, 12-09b, 12-09c, 12-10b, 12-11, and 12-12) and a well screened above the bedrock contact in the AWTF area, the Line Creek stream elevation, and the overburden-bedrock contact (Fig. 5). These seven wells represented continuously saturated locations within the basal alluvial aquifer. No notable differences in the distribution of equipotential lines were observed between

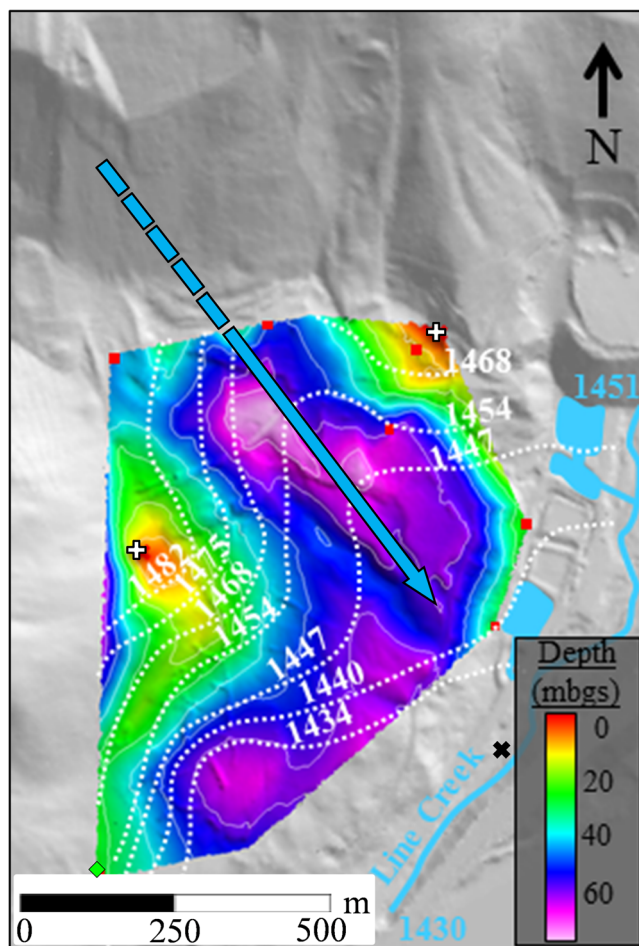


Fig. 5 Depth to bedrock map (m bgs) and contours of the annual mean hydraulic head values (white dotted line; m asl) for the basal alluvial aquifer. Contours were constructed using six wells in this study (red squares) and one well drilled as part of the active water treatment facility technical study (green diamond), surface-water elevations (blue), and the interpretation of bedrock topography on groundwater flow (bedrock outcrops shown with white crosses). The dominant conceptual groundwater flow path (blue arrow) toward the Line Creek discharge zone (black cross) is shown

plots based on mean values or seasonal measurements (data not presented). The water table sloped toward Line Creek in a SSE direction and in the same direction as the slope of the bedrock surface. The water-level map also illustrated the potential for a lateral component of groundwater from the valley walls inwards toward the thalweg of the bedrock surface and then longitudinally along the thalweg toward Line Creek. The dominant groundwater flow direction along the thalweg (Fig. 5) aligned with a groundwater discharge zone identified in Line Creek by Birkham et al. (2014) using a distributed temperature sensing system placed on the stream bed. Based on this conceptualization, the dominant lateral hydraulic gradient was determined to be along the thalweg of the bedrock surface between wells 12-09c and 12-10b (Table 1; Fig. 2b). The maximum, minimum, and mean lateral hydraulic gradients between these wells were 0.12, 0.09, and 0.11, respectively. These values were consistent with the average slope of the valley and the mapped bedrock surface of approximately 0.12; however, the lateral hydraulic gradient decreased to approximately 0.06 near the discharge area near Line Creek (i.e., between 12-10b and 12-11 or 12-12; Table 1; Fig. 2b), where the saturated thickness of the basal alluvial aquifer increased.

Downward vertical hydraulic gradients were measured in the basal alluvial aquifer at every well nest (i.e., 12-07, 12-09, and 12-10; Table 1; Fig. 2b). At nest 12-07, vertical hydraulic gradients near unity were recorded between the overburden and bedrock, suggesting the basal alluvial aquifer was perched atop the low- K bedrock at this location, albeit for only 3–4 months/year when the overburden well contained water (12-07c). At nests 12-09 and 12-10, confining layers locally separated the basal alluvial aquifer into two zones (i.e., a lower confined zone and an upper unconfined zone) or separated the basal alluvial aquifer from the underlying bedrock aquifer. The hydraulic gradients across the 2-m thick silty-clay confining layer at nest 12-09 ranged from 0.07 to 0.26 in a downward direction (between wells 12-09c and 12-09b). At nest 12-10, downward hydraulic gradients ranging from 0.02 to 0.22 were measured across the sandy-silt confining layer from the overburden (well 12-10b) to the underlying bedrock (well 12-10c); however, groundwater flow across these confining layers at nests 12-09 and 12-10 (Fig. S3 of the ESM) is expected to be minimal when compared to flows within the coarse-grained basal alluvial aquifer. A lack of vertical groundwater flow was also supported by differences in the major ion composition of groundwater samples from the deeper wells 12-09b (overburden; confined) and 12-10c (bedrock; confined) and the overlying wells 12-09c and 12-10b (overburden; unconfined), which had $(\text{Na}^+ + \text{K}^+)/(\text{CO}_3^{2-} + \text{HCO}_3^-)$ -type and $\text{Ca}^{2+}/(\text{CO}_3^{2-} + \text{HCO}_3^-)$ -type waters, respectively (Szmigielski 2015).

Hydraulic heads measured in shallow monitoring wells 12-06a and 12-09d (Table 1; Fig. 2b) ranged from 1,497 to 1,506 m asl and 1,515 to 1,518 m asl, respectively, and

represented perched aquifer conditions (Fig. 4). These saturated zones formed on a shallow confining layer comprised of glacio-lacustrine deposits (4–15 m bgs) overlying the basal alluvial aquifer. The similar elevation of the rock drain culvert intake (approximately 1,500 m asl; Fig. 4) and the hydraulic heads in the perched aquifer wells suggest the rock drain and perched aquifer were hydraulically connected. The basal alluvial aquifer, at the scale of the fluvial plain, did not appear to be directly connected with the rock drain or perched aquifer although the similar timing of peak flow and maximum groundwater levels suggest a connection farther upgradient, possibly within the waste rock. In natural disconnected groundwater systems, the stream affects groundwater primarily through streambed seepage (Brunner et al. 2011; Vazquez-Sune et al. 2007); a similar mechanism is proposed between the rock drain (and perched aquifer) and the basal alluvial aquifer at the scale of the fluvial plain.

The perched aquifer well 12-06a had water present within it throughout the year. This well, located at the toe of the waste rock dump near the rock drain culvert inlet, had a large (9.4 m) range in hydraulic head values (1,496.8–1,506.2 m asl) similar to the wells in the basal alluvial aquifer. Perched conditions in well 12-09d, located further from the rock drain culvert inlet than well 12-06a, were observed for only 2–3 months/year. This well also had a smaller (<3.5 m) annual range in hydraulic head (1,514.5–1,518.0 m asl). The different head dynamics between these two wells is attributed to processes associated with flow in the rock drain (discussed further in section “Groundwater recharge dynamics and the impact of the waste rock dump on catchment scale hydrological processes”). Additional studies to confirm the groundwater dynamics of the perched aquifer system are warranted.

Discharge from the perched aquifer occurred at groundwater springs located along the steep SE slope of the catchment (Fig. 2b). The groundwater springs ranged in elevations from 1,448 to 1,473 m asl. The majority of groundwater springs flowed for only 2–3 months/year following spring freshet. However, a few springs located between 1,453 and 1,461 m asl had greater flow rates (up to 0.0031 m³/s) and flowed most of the year. These major springs are expected to represent the perched aquifer observed in shallow groundwater wells. Lithological logs from these wells show only a single interval of fine-grained sediment (i.e., confining layer), suggesting that the remaining springs that flow periodically may represent secondary localized perched aquifers formed on multiple discontinuous confining layers. Based on the observed groundwater dynamics at perched aquifer wells (e.g. 12-09d) and the measured flow rates at the springs, the groundwater flow in the perched aquifer was inferred to be a minor component of the bulk groundwater flow from the catchment.

Quantifying groundwater flow in the basal alluvial aquifer

The total discharge from the basal alluvial aquifer (Q) was estimated using Darcy's Law, the geometric mean K from all sampling locations in the overburden aquifers (3.4×10^{-5} m/s), the mean lateral hydraulic gradient (0.11), and the saturated cross sectional area for the basal alluvial aquifer through time (defined using hydraulic head values and the mapped overburden–bedrock contact; approximately 3,500 m²). The Q over the 2-year study period ranged from 0.011 m³/s in the winter to 0.021 m³/s in the spring, with an average of 0.013 m³/s.

The total discharge from the basin through the rock drain in 2013 and 2014 was 2.61 and 2.23 Mm³/year, respectively. Based on the average Q , groundwater accounted for approximately 15% of the discharge from the basin (Q plus rock drain flow and assuming the contribution from the shallow fractured bedrock and perched aquifer are negligible) over the 2 years of study. If K values representing 1SD of the geometric mean K (3.85×10^{-6} and 3.00×10^{-4} m/s) are used to calculate Q , it could range from 0.0014 to 0.11 m³/s or < 2 to 60% of the total water discharged from the basin.

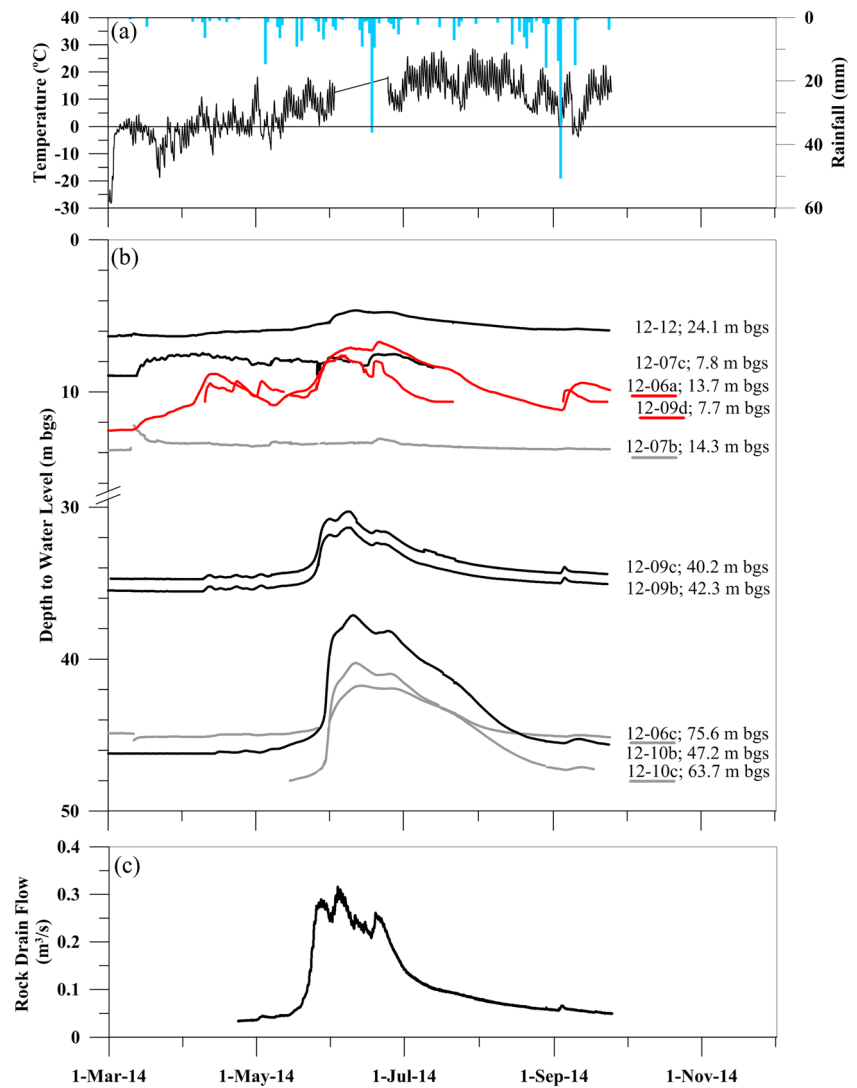
The mean groundwater velocity (v) was calculated to be 1.2×10^{-5} m/s (1.1 m/day) using the arithmetic mean n_T from all core samples from the overburden sediments (0.30) and the parameters used to calculate Q over the 2-year period as aforementioned. This yielded a travel time of 2 years for groundwater to flow from the toe of the waste rock dump to the Line Creek discharge zone defined by Birkham et al. (2014), a distance of approximately 650 m. This estimated residence time is consistent with ³He/³H groundwater ages (\pm age error) from three groundwater samples: 0.8 ± 0.5 , 1.2 ± 0.5 , and 2.8 ± 0.7 years for samples collected from 12-09c, 12-11, and 12-12, respectively (Table 1; Fig. 2b).

Groundwater recharge dynamics and the impact of the waste rock dump on catchment scale hydrological processes

The impacts of the waste rock dump on water release from the catchment (i.e., through groundwater and the rock drain) were explored in two steps. First, the hydrological response timing of groundwater and the rock drain to spring freshet was evaluated. Second, the statistical relationship between groundwater levels and rock-drain-flow hydrographs was defined.

Groundwater hydrograph responses demonstrated that shallow groundwater in the fluvial plain (< 12 m bgs) responded sooner to spring freshet (March–April) than deeper groundwater and the rock drain (Fig. 6). This is attributed to local recharge resulting from earlier snowmelt at lower elevations, which appears more pronounced near the dump (i.e., 12-06a and 12-09d) than at greater distances (e.g., well 12-04 in the AWTF area; Fig. 4); for example, lower elevation

Fig. 6 Groundwater responses to the spring-freshet in 2014: **a** air temperatures (solid line) and daily total rainfall (blue vertical bars); **b** hydrographs from the basal alluvial aquifer (black), perched aquifer (red), the bedrock formation (grey) shown with text (underlined with the corresponding color for perched and bedrock aquifer hydrographs) presenting the depth of the bottom of the screen intake zone (m bgs); and **c** surface-water flow in the rock drain



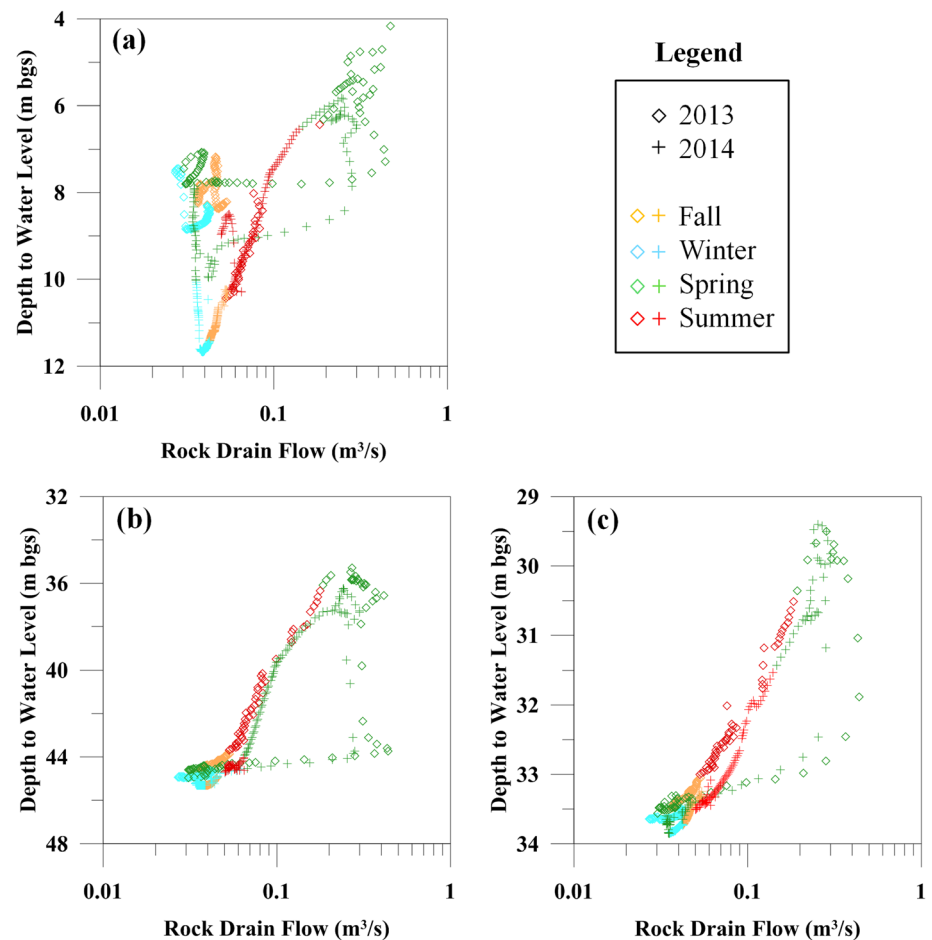
snowmelt caused a large water-level increase (+ 1.6 m) in well 12-06a between March 16 and April 1, 2014 but water levels in shallow wells at greater distances from the dump, the rock drain flow rate, and deeper groundwater levels remained unchanged. The lack of response by deep groundwater and the rock drain demonstrates that early season snowmelt likely has a limited impact on catchment-scale hydrological processes. Further, the water storage threshold of the shallow zone (i.e., unsaturated and saturated, <12 m bgs) is more easily exceeded than other components of the hydrologic system (e.g., deep groundwater).

The relationship between groundwater levels and rock drain flow was explored to assess groundwater recharge dynamics using the timing of recharge events and the time lags associated with these events in the overburden aquifers. Relationships were examined by using hysteresis plots and cross-correlation. The hysteresis plots compared groundwater level and rock drain flow (log-scale) each day over the two hydrological years for monitoring locations with sufficiently

complete datasets. Cross correlation was conducted with the same representative monitoring location hydrographs using the cross correlation function (CCF) in the R statistics program (R Development Core Team 2006). These data were used to demonstrate the degree of fidelity between the two variables and the correlation between two variables at specific time lags (Allen et al. 2010).

The relationship between groundwater levels and rock drain flow was hysteretic, demonstrating that the dominant hydrological processes differed between the annual recharge and recession periods (Fig. 7). This loop structure, attributed to the time delay between changes in water level and changes in rock drain flow, is generally consistent with other snowmelt-driven groundwater systems that are unaffected by mining in BC (cf. Allen et al. 2010). The hysteresis pattern in the late spring and summer in the perched aquifer is counter-clockwise year-to-year and is consistent with that of the basal aquifer. However, marked irregularities exist in the perched aquifer for the remainder of the year (Fig. 7a). An atypical

Fig. 7 Hysteresis plots of depth to water level in the perched aquifer well **a** 12-06a and the basal alluvial aquifer wells **b** 12-10b and **c** 12-09c plotted vs. rock drain flow (log scale). Results are divided into Fall (October–December), Winter (January–March), Spring (April–June), and Summer (July–September) for the 2013 and 2014 hydrological years



clockwise loop structure is noted in the early spring (March–April) and also during late summer (2014) and early fall (2013) rainfall events. These events produced large water-level responses in shallow groundwater (<12 m bgs), demonstrating that the water storage threshold in the shallow aquifers is more easily exceeded regardless of timing within the recession period of the annual hydrograph. Fovet et al. (2015) show that the non-linear relation between groundwater levels and stream flow in catchments results from the manifestation of storage thresholds occurring in the catchment runoff processes.

Based on the hysteresis plots, it appears that secondary hydrological processes at the local scale serve to desynchronize shallow groundwater levels in the perched aquifer from the rock drain. This is supported by cross correlation of representative hydrographs, which demonstrate that the greatest waveform synchronicity between groundwater and the rock drain occurs in progressively deeper overburden wells (i.e., basal alluvial aquifer; data not presented)—for example, the strongest waveform fidelity ($R^2 = 0.90$) occurs between the rock drain and well 12-10b (170 m from subsurface intake of the culvert and mid-screen depth of 45.7 m bgs; Table 1; Fig. 2b) hydrographs when a lag time of 9 days was

applied to the well hydrograph (Fig. 4). This strong correlation could suggest a connection between the basal alluvial aquifer and rock drain upgradient of the study site (i.e., beneath the waste rock dump). A connection is also supported by the similar water type of the basal aquifer at certain locations (e.g., wells 12-10b, 12-11, and 12-12) and the rock drain [$\text{Mg}^{2+}/(\text{Ca}^{2+})/(\text{SO}_4^{2-})$ type water] (Szmigielski 2015).

Although the timing of spring freshet across the catchment and similar water types at certain locations may suggest there is some connection between the rock drain and deeper groundwater, observations from rainfall events suggest that groundwater recharge occurs primarily as *direct* recharge (i.e., widespread percolation of precipitation directly to the aquifers) as opposed to *indirect* recharge via the rock drain. Several large rainfall events (with known water inputs) in 2013 (June 18–20) and 2014 (June 16–18 and September 2–3) produced marked responses in deep groundwater located below thick unsaturated profiles and in the rock drain (Figs. 4 and 6). Observations of the groundwater level changes highlights that the magnitude and timing of the groundwater response was consistent with a rise in water level governed by specific yield and a delay due to propagation of the pressure wave associated with the recharging water across the unsaturated zone. The

magnitude of the groundwater level rise was consistent with the observed magnitudes of the rainfall events for a specific yield in the range of 0.01–0.13 as per the water-table fluctuation method (Healy and Cook 2002). This range of specific yield is consistent with the minimum values for materials ranging from fine sand and to coarse gravel (0.10–0.12) as reported by Johnson (1967). Further, the time delay in the deep groundwater level responses to the rainfall events was consistent with estimates of the velocity of an infiltration front as described by Smith (1993), in which the magnitude of the increase in volumetric water content was in the range of 0.01–0.03. These observations support the suggestion that although the average water levels within the basal aquifer are due to the lateral transmission of groundwater from upstream of the study area towards Line Creek, the dynamics in the water levels are most likely due to the dynamics in local recharge over the study site as a result of rainfall or snowmelt infiltration. Allen et al. (2010) state that aquifer-stream systems that are snowmelt-dominated (i.e., nival regimes) and *direct* recharge-driven, are common in upland areas of southeastern BC.

A detailed interpretation of the impact of the dump on hydrological processes was undertaken by Villeneuve et al. (2017) using valley wide annual water balances. The evaluation conducted in this study suggests the historic stream (and current rock drain) is predominately a ‘losing’ stream in the fluvial sediments. The interaction between the shallow groundwater system and the rock drain is supported by several observations. These include the fact that the rock drain produced the large seasonal variations in water levels in the perched aquifer (12-06a) directly at the toe of the dump (9.4 m; 1,496.8–1,506.2 m asl) and that the continuously saturated conditions at well 12-06a were not observed in the other perched aquifer wells (i.e., 12-09d and AWTF 12-04; Table 1; Figs. 2b and 4) or in the discontinuous outflows from perched aquifer groundwater springs (discussed in section “Hydraulic heads and rock drain flow”). Furthermore, an interaction between the shallow groundwater flow system and the rock drain is consistent with the similarity of the major ion composition of water in well 12-06a and the rock drain [$\text{Mg}^{2+}/(\text{Ca}^{2+})/(\text{SO}_4^{2-})$ type water] vs. shallow groundwater further from the dump (e.g., AWTF 12-04; $\text{Ca}^{2+}/(\text{CO}_3^{2-} + \text{HCO}_3^-)$ water type; Fig. 4 (Szmigielski 2015)).

Summary and conclusions

The hydrogeology of a stratigraphically complex valley-bottom groundwater system in a 10-km² headwater catchment covered by 2.7 km² of coal waste rock was characterized using lithologies, n_T , hydraulic gradients, K , and seasonal responses of rock drain discharge and groundwater levels to the local hydroclimate. The valley-bottom sediments were composed

of glacial and melt water successions (up to 64 m thick) deposited as a series of cut and fill structures in a U-shaped valley. Groundwater discharge from the catchment to Line Creek was dominated by flow from a high- K (3.4×10^{-5} m/s) unconfined aquifer at the base of the unconsolidated overburden sediments (i.e., the basal alluvial aquifer), with its lower boundary formed by the underlying low- K (3.3×10^{-8} m/s) shale of the Fernie Formation. Discharge through the basal alluvial aquifer doubled in response to spring freshet and the saturated thickness varied by up to 10.4 m annually due to focused flow in the thalweg of the bedrock surface. A minor component of outflow from the catchment occurred in a perched aquifer unit formed on shallow fine-grained glacio-lacustrine sediments (5–15 m bgs). Data suggest the perched aquifer and rock drain are not hydraulically connected with the underlying basal alluvial aquifer. Residence time in the basal alluvial aquifer across the 650-m flow path from the toe of the dump to a discharge point at Line Creek is rapid (<3 years). The basal alluvial aquifer discharged approximately 15% of the total water from the catchment over the 2-year study period.

Based on groundwater level and rock drain flow responses to hydroclimate, the rock drain-groundwater system is defined by a seasonal response to snowmelt (nival regime) dominated by *direct* recharge across the catchment. The basal alluvial aquifer water-level map and bedrock topography suggest longitudinal (down-valley) and lateral (cross-valley) groundwater recharge mechanisms. The water-level dynamics (shown on hysteresis plot) of the perched aquifer in proximity to the waste rock dump appear to be impacted by rock drain-groundwater interaction. Although additional quantification is required, the waste rock dump appears to increase the discharge through the shallow perched aquifer.

Acknowledgements The authors thank Rob Klein and Tim Chala at Teck Resources Ltd. Line Creek Operation for technical assistance and logistical support during field work. Several figures were created with the help of Stephanie Villeneuve.

Funding information Financial support was provided by Teck Resources Ltd. and an NSERC Industrial Postgraduate Scholarship (JS).

References

- Ajami H, Meixner T, Dominguez F, Hogan J, Maddock T (2012) Seasonalizing mountain system recharge in semi-arid basins: climate change impacts. *Groundwater* 50:585–597. <https://doi.org/10.1111/j.1745-6584.2011.00881.x>
- Allen DM (2011) Climate change impacts in valley-bottom aquifers in mountain regions: case studies from British Columbia, Canada. In: Treidel H., Martin-Bordes JL, Gurdak JJ (eds) *Climate change effects on groundwater resources: a global synthesis of findings and recommendations*. IAH International Contributions to Hydrogeology, CRC, Boca Raton, FL, 414 pp
- Allen DM, Whitfield PH, Werner A (2010) Groundwater level responses in temperate mountainous terrain: regime classification, and

- linkages to climate and streamflow. *Hydrol Proc* 24(23):3392–3412. <https://doi.org/10.1002/hyp.7757>
- American Society for Testing and Materials (ASTM) (2007) D422–63: standard test method for particle-size analysis of soils. ASTM International, West Conshohocken, PA
- American Society for Testing and Materials (ASTM) (2008) D4044–96: Standard test method for (field procedure) for instantaneous change in head (slug) tests for determining hydraulic properties of aquifers. ASTM International, West Conshohocken, PA
- American Society for Testing and Materials (ASTM) (2009) D7263–09: Standard test methods for laboratory determination of density (unit weight) of soil specimens. ASTM International, West Conshohocken PA. <https://doi.org/10.1520/D7263-09>
- American Society for Testing and Materials (ASTM), 2010. D2216–10 (2010) Standard test methods for laboratory determination of water (moisture) content of soil and rock by mass. ASTM International, West Conshohocken, PA. <https://doi.org/10.1520/D2216-10.N>
- Barbour SL, Hendry MJ, Carey SK (2016) High-resolution profiling of the stable isotopes of water in unsaturated coal waste rock. *J Hydrol* 534:616–629. <https://doi.org/10.1016/j.jhydrol.2016.01.053>
- Bernhardt ES, Palmer MA (2011) The environmental costs of mountain-top mining valley fill operations for aquatic ecosystems of the central Appalachians. *Ann N Y Acad Sci* 1223(1):39–57. <https://doi.org/10.1111/j.1749-6632.2011.05986.x>
- Birkham T, Barbour SL, Goodbrand A, Tallon L, Szmigielski J, Klein R (2014) Assessing groundwater discharge to streams with distributed temperature sensing technology. Presented at the 2014 British Columbia Technical and Research Committee on Reclamation Symposium, Prince George, BC, September 2015
- Bouwer H, Rice RC (1976) A slug test for determining hydraulic conductivity of unconfined aquifers with completely or partially penetrating wells. *Water Resour Res* 12(3):423–428
- Brunner P, Cook PG, Simmons CT (2011) Disconnected surface water and groundwater: from theory to practice. *Ground Water* 49(4):460–467. <https://doi.org/10.1111/j.1745-6584.2010.00752.x>
- Butler JJ, Garnett EJ, Healey JM (2003) Analysis of slug tests in formations of high hydraulic conductivity. *Groundwater* 41(5):620–631
- Butrenchuk SB (1987) Phosphate in southeastern British Columbia. Open file report 1987-16, BC Ministry of Energy, Mines and Petroleum Resources, Victoria, 103 pp
- Clow DW, Schrott L, Webb R, Campbell DH, Torizzo A, Domblaser M (2003) Ground water occurrence and contributions to streamflow in an alpine catchment. *Colorado Front Range Ground Water* 41(7): 937–950. <https://doi.org/10.1111/j.1745-6584.2003.tb02436.x>
- De Geer G (1912) A geochronology of the last 12,000 years. Proceedings of the International Geological Congress, Stockholm, 1912, pp 241–253
- Dreher G, Finkelman R (1992) Selenium mobilization in a surface coal mine, Powder River basin, Wyoming, USA. *Environ Geol Water Sci* 19(3):155–167
- Driscoll FG (1986) *Groundwater and wells*, 2nd edn. Johnson Filtration Systems, St. Paul, MN
- Environment Canada (2017) Historical data: Weather Station ID 1157630. http://climate.weather.gc.ca/historical_data/search_historic_data_e.html. Accessed January 2017
- Eshel G, Levy GJ, Mingelgrin U, Singer MJ (2002) Critical evaluation of the use of laser diffraction for particle-size distribution analysis. *Soil Sci Soc Am J* 68:736–743
- Everett LG (1985) *Groundwater monitoring handbook for coal and oil shale development*. Elsevier, New York
- Fovet O, Ruiz L, Hrachowitz M, Fauchoux M, Gascuel-Oudoux C (2015) Hydrological hysteresis and its value for assessing process consistency in catchment conceptual models. *Hydrol Earth Syst Sci* 19(1): 105. <https://doi.org/10.5194/hess-19-105-2015>
- Gardner P, Solomon DK (2009) An advanced passive diffusion sampler for the determination of dissolved gas concentrations. *Water Resour Res* 45:W06423. <https://doi.org/10.1029/2008WR007399>
- Golder Geotechnical Consultants Ltd. (now Golder Associates Ltd.) (1979) Geotechnical investigations for plant site and related facilities Line Creek coal project. Golder, Calgary, AB
- Griffith MB, Norton SB, Alexander LC, Pollard AI, LeDuc SD (2012) The effects of mountaintop mines and valley fills on the physico-chemical quality of stream ecosystems in the central Appalachians: a review. *Sci Total Environ* 417–418:1–12. <https://doi.org/10.1016/j.scitotenv.2011.12.042>
- Halford KJ, Kuniansky EL (2002) Documentation of spreadsheets for the analysis of pumping-aquifer test and slug test data. US Geol Surv Open-File Rep 02-197. <http://pubs.usgs.gov/of/2002/ofr02197/>. Accessed June 2018
- Healy RW, Cook PG (2002) Using groundwater levels to estimate recharge. *Hydrogeol J* 10:91. <https://doi.org/10.1007/s10040-001-0178-0>
- Hendry MJ, Biswas A, Essilfie-Dughan J, Chen N, Day SJ, Barbour SL (2015) Reservoirs of selenium in coal waste rock: Elk Valley, British Columbia, Canada. *Environ Sci Technol* 49(13):8228–8236. <https://doi.org/10.1021/acs.est.5b01246>
- Heusser CJ (1956) Postglacial environments in the Canadian Rocky Mountains. *Ecol Soc Am* 26(4):263–282
- Holzman DC (2011) Mountaintop removal mining: digging into community health concerns. *Environ Health Perspect* 119(11):A476–A583
- Johnson AI (1967) Specific yield: compilation of specific yields for various materials. US Geol Surv Water-Suppl Pap 1662-D, 74 pp
- Jorgensen F, Sandersen PBE (2006) Buried and open tunnel valleys in Denmark: erosion beneath multiple ice sheets. *Quatern Sci Rev* 25(11–12):1339–1363. <https://doi.org/10.1016/j.quascirev.2005.11.006>
- Loke MH, Dahlin T (2002) A comparison of the Gauss-Newton and quasi-Newton methods in resistivity imaging inversion. *J Appl Geophys* 49:149–162
- Manning AH, Solomon DK (2003) Using noble gases to investigate mountain-front recharge. *J Hydrol* 275(3–4):194–207. [https://doi.org/10.1016/S0022-1694\(03\)00043-X](https://doi.org/10.1016/S0022-1694(03)00043-X)
- Manning AH, Solomon DK (2005) An integrated environmental tracer approach to characterizing groundwater circulation in a mountain block. *Water Resour Res* 41(12):1–18. <https://doi.org/10.1029/2005WR004178>
- Michael K, Bachu S (2001) Origin and evolution of formation waters in the west-central part of the Alberta Basin. Canadian Society of Petroleum Geologists. Rock the Foundation Convention, Edmonton, AB, June 18–22, 2001, pp 1–5
- Miller AJ, Zégre NP (2014) Mountaintop removal mining and catchment hydrology. *Water (Switzerland)* 6(3):472–499. <https://doi.org/10.3390/w6030472>
- Mira Geosciences Ltd. (2009) Mira GOCAD® Mining Suite software version 2009.4. Software available from <http://www.mirageoscience.com/ourproducts/software-product/gocad-mining-suite>. Accessed June 2018
- Naftz D, Rice J (1989) Geochemical processes controlling selenium in ground water after mining, Powder River basin, Wyoming, USA. *Appl Geochem* 4(1983):565–575. <http://www.sciencedirect.com/science/article/pii/088329278990067X>
- R Development Core Team (2006) R: a language and environment for statistical computing. R Foundation for Statistical Computing, Vienna, Austria. <http://www.R-project.org>. Accessed June 2018
- Riddell J (2012) Potential for freshwater bedrock aquifers in Northeast British Columbia: regional distribution and lithology of surface and shallow subsurface bedrock units (NTS 093I, O, P; 094A, B, G, H, I, J, N, O, P). In: *Geoscience reports 2012*, British Columbia Ministry of Energy and Mines, Victoria, pp 65–78

- Rosenshein JS (1988) Region 18, alluvial valleys. In: Back W, Rosenshein JS, Seaber PR (eds) *Hydrogeology: the geology of North America*, v. O-2. Geological Society of America, Boulder, CO
- Roy JW, Hayashi M (2009) Multiple, distinct groundwater flow systems of a single moraine–talus feature in an alpine watershed. *J Hydrol* 373(1):139–150
- Russell HJ, Hinton MJ, van der Kamp G, Sharpe DR (2004) An overview of the architecture, sedimentology and hydrogeology of buried-valley aquifers in Canada. In: *Proceedings of the 57th Canadian Geotechnical Conference and the 5th Joint CGS-IAH Conference*, October 2004, Quebec, Canadian Geotechnical Society, pp 26–33
- Shatilla NJ (2013) *The influence of surface mining on runoff timing and flow pathways in Elk Valley, British Columbia*. McMaster University, Hamilton, ON
- Sperazza M, Moore JN, Hendrix MS (2004) High-resolution particle size analysis of naturally occurring very fine-grained sediment through laser diffractometry. *J Sediment Res* 74(5):736–743
- SRK Consulting (Canada) Inc. (2013) *Teck 2012 Line Creek AWTF residuals landfill site: ongoing monitoring and hydrogeological investigation*. Teck Coal, Vancouver, BC
- Szmigielski J (2015) *Characterizing a groundwater system downgradient of a coal mine waste rock dump, Elk Valley, British Columbia, Canada*. MSc Thesis, University of Saskatchewan, Saskatoon, SK, Canada
- Teck Resources Ltd. (2017) *Teck area based management plan*. Available at <http://www2.gov.bc.ca/gov/content/environment/waste-management/industrial-waste/mining-smelting/teck-area-based-management-plan>. Accessed 4 September 2017
- Tiedeman CR, Goode DJ, Hsieh PA (1998) Characterizing a ground water basin in a New England mountain and valley terrain. *Ground Water* 36(4):611–620. <https://doi.org/10.1111/j.1745-6584.1998.tb02835.x>
- Vazquez-Sune E, Capino B, Abarca E, Carrera J (2007) Estimation of recharge from floods in disconnected stream–aquifer systems. *Ground Water* 45(5):579–589. <https://doi.org/10.1111/j.1745-6584.2007.00326.x>
- Villeneuve SA, Barbour SL, Hendry MJ, Carey SK (2017) Estimates of water and solute release from a coal waste rock dump in the Elk Valley, British Columbia, Canada. *Sci Total Environ* 601–602:543–555. <https://doi.org/10.1016/j.scitotenv.2017.05.040>
- Viviroli D, Messerli B (2003) Assessing the hydrological significance of the world’s mountains. *Mount Res Dev* 23(4):369–375. [https://doi.org/10.1659/0276-4741\(2003\)023](https://doi.org/10.1659/0276-4741(2003)023)
- Viviroli D, Hans HD, Messerli B, Meybeck M, Weingartner R (2007) Mountains of the world, water towers for humanity: typology, mapping, and global significance. *Water Resour Res* 43:1–13. <https://doi.org/10.1029/2006WR005653>
- Wahi AK, Hogan JF, Ekwurzel B, Baillie MN, Eastoe CJ (2008) Geochemical quantification of semiarid mountain recharge. *Ground Water* 46(3):414–425. <https://doi.org/10.1111/j.1745-6584.2007.00413.x>
- Wellen CC, Shatilla NJ, Carey SK (2015) Regional scale selenium loading associated with surface coal mining, Elk Valley, British Columbia, Canada. *Sci Total Environ* 532(June):791–802. <https://doi.org/10.1016/j.scitotenv.2015.06.040>
- Wilson JL, Guan H (2004) Mountain-block hydrology and mountain-front recharge. In: Hogan JF et al. (eds) *Groundwater recharge in a desert environment: the southwestern United States*. Water Science and Application, Series 9, AGU, Washington, DC, pp 113–137
- Winter TC, Rosenberry DO, LaBaugh JW (2003) Where does the ground water in small catchment come from? *Ground Water* 41(7):989–1000. <https://doi.org/10.1111/j.1745-6584.2003.tb02440.x>
- Zonge K, Wynn J, Urquhart S (2005) Resistivity, induced polarization and complex resistivity. In: Butler DK (ed) *Near surface geophysics*. SEG, Tulsa, OK, pp 265–300